Electronic Supplementary Material (ESI) for Sustainable Energy & Fuels.
This journal is © The Royal Society of Chemistry 2017

Supplemental Material for: 'Candidate photoferroic absorber materials for thin-film solar cells from naturally occurring minerals: enargite, stephanite, and bournonite'

Suzanne K. Wallace[a,b], Katrine L. Svane[a], William P. Huhn[c], Tong Zhu[c], David B. Mitzi[c,d], Volker Blum[c], and Aron Walsh*[b,e]

[a] *Department of Chemistry, Centre for Sustainable Chemical Technologies, University of Bath, Claverton Down, Bath, BA2 7AY, UK*

[b] *Department of Materials, Imperial College London, Exhibition Road, London SW7 2AZ, UK. Email: a.walsh@imperial.ac.uk*

[c] *Department of Mechanical Engineering and Materials Science, Duke University, Durham, North Carolina 27708, USA*

[d] *Department of Chemistry, Duke University, Durham, North Carolina 27708, USA*

[e] *Global E^3 Institute and Department of Materials Science and Engineering, Yonsei University, Seoul 03722, Korea*

1 Total energy convergence for geometry optimization

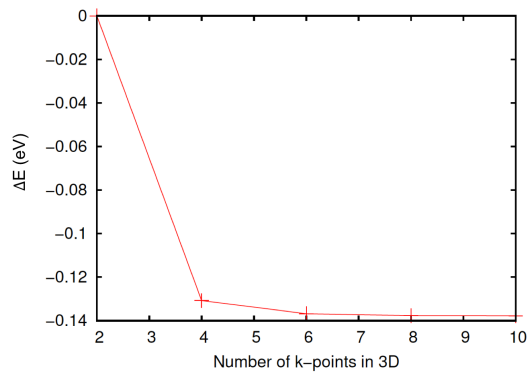

Figure 1: Convergence of the change in calculated total energy for enargite (Cu_3AsS_4) with respect to the number of k-points, calculated using the PBE functional.

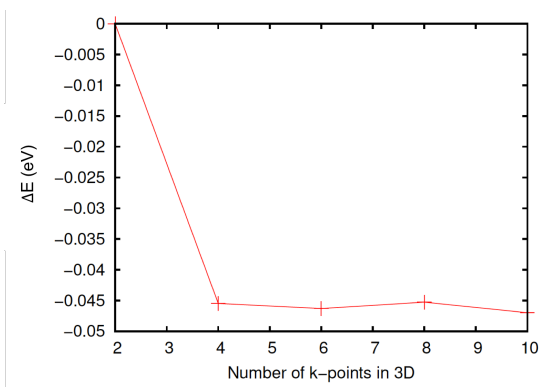

Figure 2: Convergence of the change in calculated total energy for bournonite ($CuPbSbS_3$) with respect to the number of k-points, calculated using the PBE functional.

2 Convergence of band structure

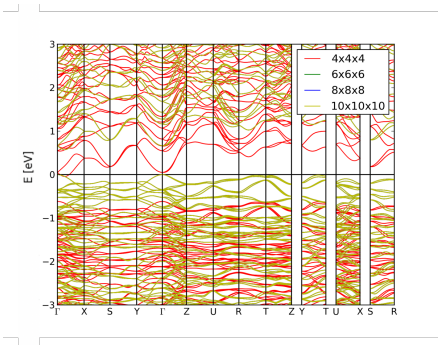

Figure 3: Convergence of bournonite band structure with increased density of k-points using a tight basis set calculated using PBE+SOC. Note that these calculations were performed for a different orientation of the unit cell as in the main body of the paper.

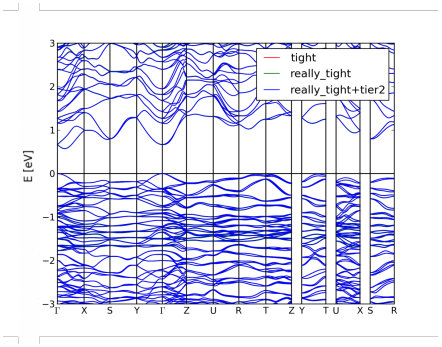

Figure 4: Convergence of bournonite band structure with increased basis set using an $8 \times 8 \times 8$ k-grid calculated using PBE+SOC. Note that these calculations were performed for a different orientation of the unit cell as in the main body of the paper.

3 Convergence of DOS

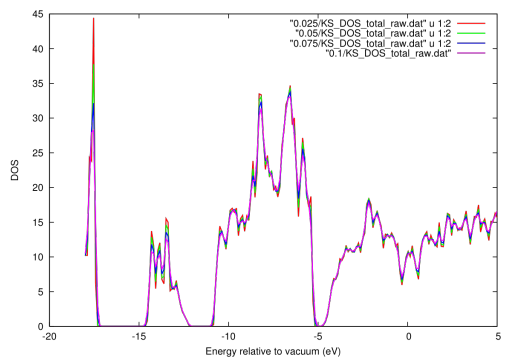

Figure 5: Convergence of bournonite density of states (DOS) with respect to Gaussian broadening applied to obtain a smooth density of states based on the peaks produced by individual states. Calculations were performed with an $8 \times 8 \times 8$ k-grid using PBE+SOC.

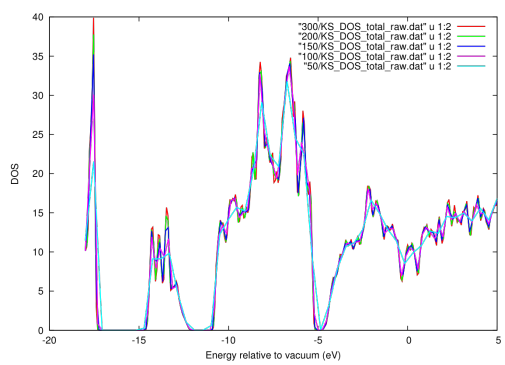

Figure 6: Convergence of bournonite density of states (DOS) with respect to the number of energy data points for which the DOS is given. Calculations were performed with an $8 \times 8 \times 8$ k-grid using PBE+SOC.

4 Fits to band extrema for effective mass calculation

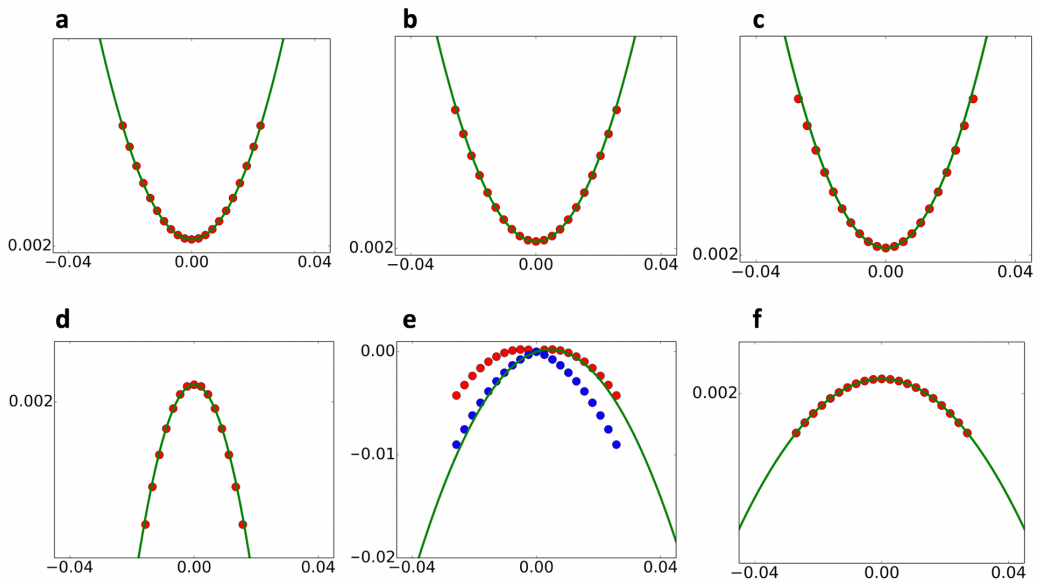

Figure 7: Parabolic fits to the band extrema of enargite (Cu_3AsS_4), where a-c correspond to the conduction band minimum (CBM) in directions ||a, ||b and ||c respectively and d-f correspond to the valence band maximum (VBM) in directions ||a, ||b and ||c respectively. Red dots are the band energies or eigenvalues, ϵ(k), green continuous curves are parabolic fits to these values, E(k). For the VBM in ||b direction, the extrema of the parabola did not coincide with the VBM for the data points. In this case we allow the fitting procedure to locate the position of the VBM and corresponding k-points. To check the extrapolated fitting curve, the DFT-HSE06+SOC ϵ(k) of the lower band (blue dots) are also shown for the VBM in the ||b direction.

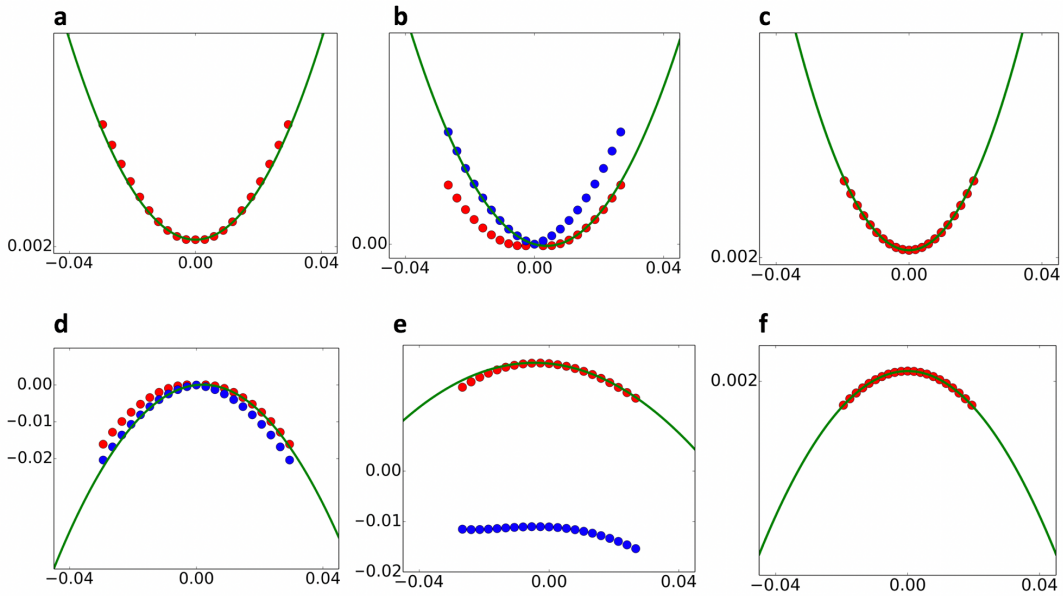

Figure 8: Parabolic fits to the band extrema of stephanite (Ag_5SbS_4), where a-c correspond to the conduction band minimum (CBM) in directions ||a, ||b and ||c respectively and d-f correspond to the valence band maximum (VBM) in directions ||a, ||b and ||c respectively. Red dots are the band energies or eigenvalues, ϵ(k), green continuous curves are parabolic fits to these values, E(k). For the VBM in ||a and ||b directions, the extrema of the parabola did not coincide with the VBM for the data points. In this case we allow the fitting procedure to locate the position of the VBM and corresponding k-points. To check the extrapolated fitting curve, the DFT-HSE06+SOC ϵ(k) of the lower band (blue dots) are also plotted. Similarly, for the CBM in the ||b direction the extrema of the parabola did not coincide with the CBM for the data points. We again allow the fitting procedure to locate the position of the CBM and corresponding k-points. To check the extrapolated fitting curve, the DFT-HSE06+SOC ϵ(k) of the lower band (blue dots) are also plotted.

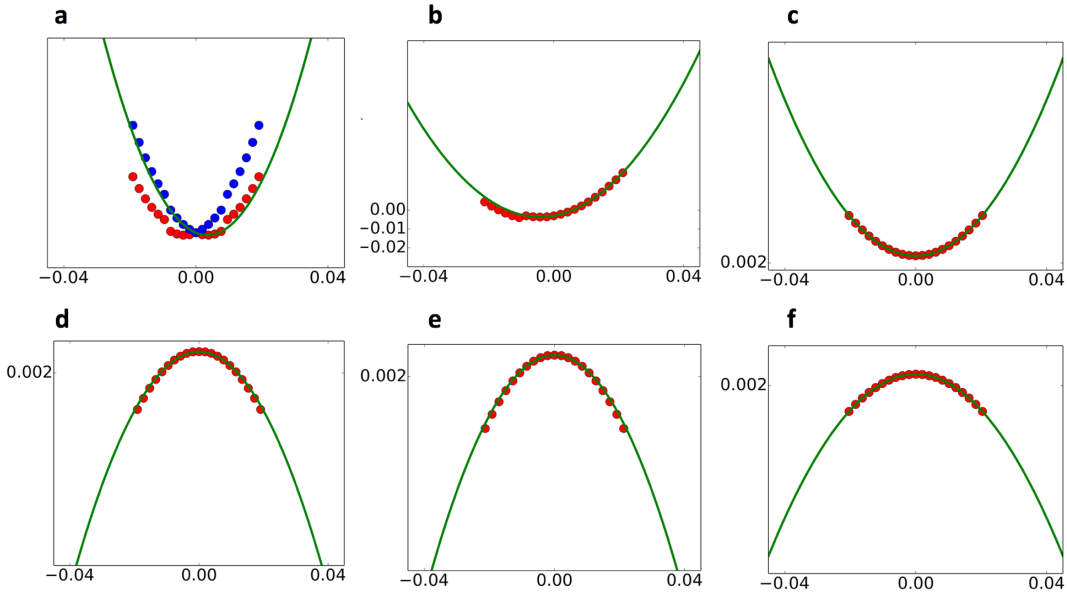

Figure 9: Parabolic fits to the band extrema of bournonite ($CuPbSbS_3$), where a-c correspond to the conduction band minimum (CBM) in directions ||a, ||b and ||c respectively and d-f correspond to the valence band maximum (VBM) in directions ||a, ||b and ||c respectively. Red dots are the band energies or eigenvalues, ϵ(k), green continuous curves are parabolic fits to these values, E(k). For the CBM in ||a direction, the extrema of the parabola did not coincide with the CBM for the data points. In this case we allow the fitting procedure to locate the position of the CBM and corresponding k-points. To check the extrapolated fitting curve, the DFT-HSE06+SOC ϵ(k) of the upper band (blue dots) are also shown for the CBM in the ||a direction.

5 Convergence of dielectric functions

We perform a convergence test for the optical dielectric function of bournonite ($CuPbSbS_3$) using the PBE functional. It was only possible to carry out the convergence test with PBE for bournonite, as both stephanite and enargite do not possess a band gap at this level of theory. From this we find the dielectric function of bournonite to converge with a k-point grid of density 8x8x8, as shown in figure 10. However, the smaller unit cells and lower valence band DOS of enargite and stephanite could indicate that these materials may require a more dense k-point grid than for bournonite. Therefore for enargite and stephanite a subsequent convergence test was carried out at the HSE level of accuracy, as shown in figures 11 and 12, where it was found that both materials required a 10x10x10 k-point grid for a converged dielectric function. All calculations for the optical dielectric function were performed using the FHI-aims software package.

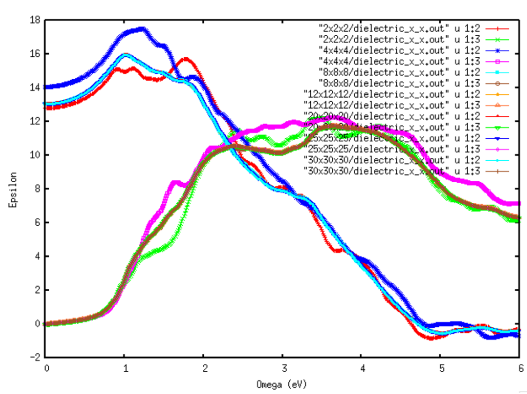

Figure 10: Convergence of the calculated dielectric function of bournonite ($CuPbSbS_3$), calculated with the PBE functional and SOC, with respect to the density of the k-point grid.

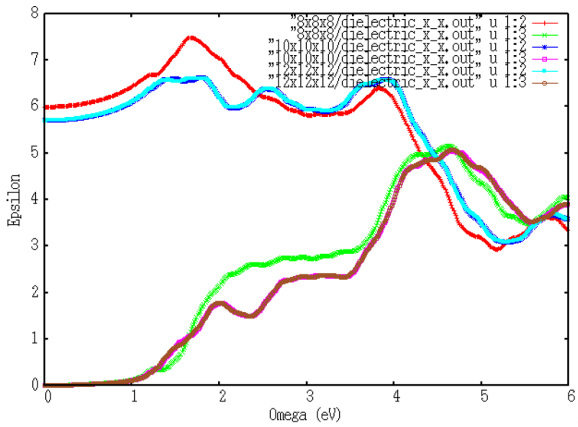

Figure 11: Convergence in the calculated optical dielectric function of enargite (Cu_3AsS_4), calculated with the HSE functional and SOC, with respect to the density of the k-point grid.

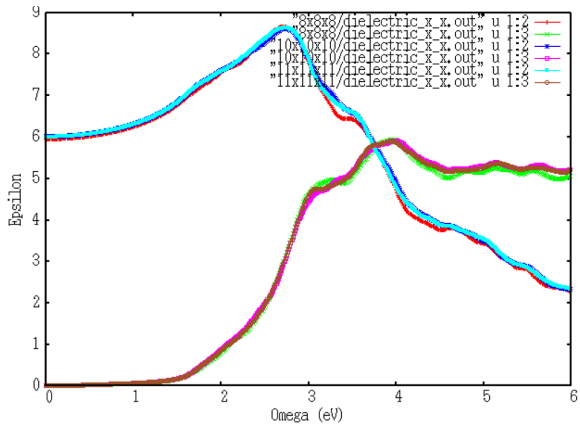

Figure 12: Convergence in the calculated optical dielectric function of stephanite (Ag_5SbS_4), calculated with the HSE functional and SOC, with respect to the density of the k-point grid.

6 Derivation of units of the absorption coefficient

The complex dielectric function is given by equation 1.

$$\underline{\epsilon} = \epsilon + i\tilde{\epsilon} \tag{1}$$

The extinction coefficient is given by equation 2, where $|\underline{\epsilon}|$ is given by equation 3.

$$\kappa = \sqrt{\frac{|\underline{\epsilon}| + \epsilon}{2}} \tag{2}$$

$$|\underline{\epsilon}| = \sqrt{\epsilon^2 + \tilde{\epsilon}^2} \tag{3}$$

The absorption coefficient is given by equation 4. $\frac{1}{\lambda}$ can be obtained from equation 5, where ω is the energy of the incident photon, to give the expression for α in equation 6

$$\alpha = \frac{4\pi\kappa}{\lambda} \tag{4}$$

$$\omega = \frac{hc}{\lambda} \tag{5}$$

$$\alpha(\omega) = \frac{4\pi}{hc}\omega\sqrt{\frac{-Re\epsilon(\omega) + \sqrt{Re^2\epsilon(\omega) + Im^2\epsilon(\omega)}}{2}} \tag{6}$$

From equation 6, we can obtain the units of the absorption coefficient. ϵ is dimensionless, the units of the α therefore are the units of $\frac{\omega}{hc}$. ω is in units of eV, Planck's constant, $h = 4.135667662 \times 10^{-15} eVs$ and the speed of light, c = 3×10^8 m s^{-1}. This gives $hc \approx 1.24 \times 10^{-6} eVm$ or $1.24 \times 10^{-4} eVcm$. Therefore α is in units of cm^{-1}.

7 Electron localisation function

The electron localisation function (ELF) [3] is calculated in VASP using the HSE06 functional and a $2 \times 2 \times 2$ k-mesh. The ELF gives the probability of finding an electron near a reference electron, and thus highlights the presence of bonds and lone pairs.

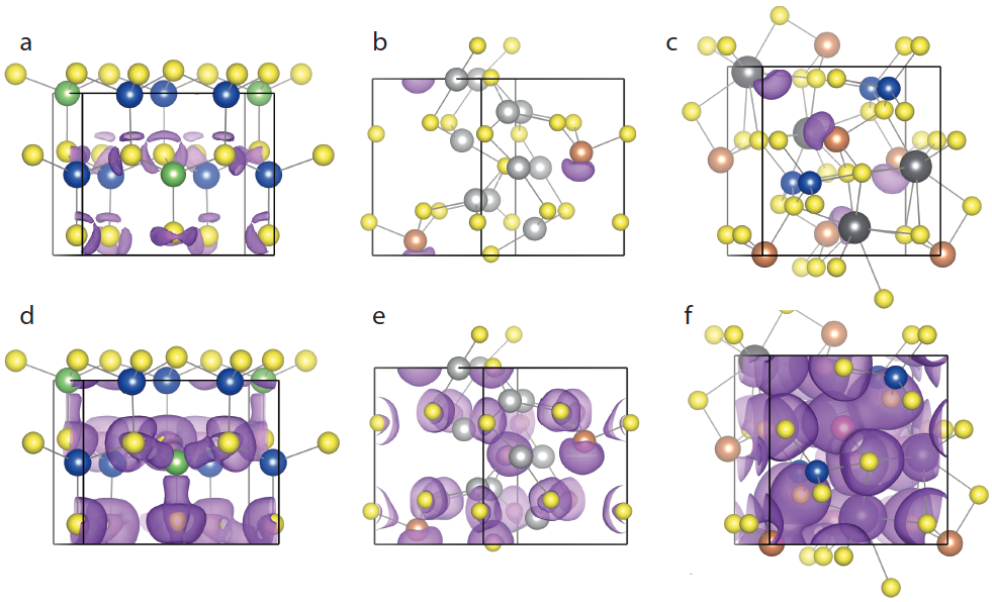

Figure 13: Electron localisation function of enargite (Cu_3AsS_4) (a and d), stephanite (Ag_5SbS_4) (b and e) and bournonite ($CuPbSbS_3$) (c and f). The values of the isosurfaces are a) 0.875, b-c) 0.925, d-e) 0.75 and f) 0.45.

The ELF is shown for enargite, bournonite and stephanite in Figure 13. At high values of the iso-surface (a-c) the lone pairs of Sb in stephanite and bournonite (b and c) are clearly seen. No lone pairs are seen for As in enargite(a), but at lower values of the ELF isosurface bonding is evident (d). The Pb atoms in bournonite do not show any lone pairs at high values of the isosurface either, but a localised spherical region around the Pb

atom is observed at lower values (f). The results for bournonite are in agreement with previous calculations [1].

8 Calculations of spontaneous lattice polarisation

Bournonite and enargite crystallise in the $Pmn2_1$ spacegroup (31), while stephanite crystallises in the $Cmc2_1$ spacegroup (36). Both of these groups have a mirror plane in the yz-plane, implying no polarisation in the x-direction and a screw axis along the z–direction, implying that polarisation is allowed along the z–direction only [2]. Indeed we can verify that the polarization is 0 along the x- and y-axes in our three structures.

To investigate the strength of polarity in the materials, calculations of the spontaneous electric polarisation, P_s, of each material were performed using the Berry-phase formalism [4] with the methodology outlined in reference [5]. Only differences in polarisation are physically meaningful, we therefore optimise the structure with polarisation $+P_s$ and invert this structure to get the opposite polarisation, $-P_s$. The polarisation difference between those two structures, $2P_s$, is calculated and we verify that the change in polarisation is continuous by also calculating the polarisation for a number of configurations connecting the two structures, with their coordinates $\mathbf{r}$ obtained from equation 7, where λ is a number between 0 and 1.

$$\mathbf{r} = \lambda \mathbf{r}_{P_s} + (1 - \lambda)\mathbf{r}_{-P_s} \tag{7}$$

Note that to make the path the atoms in the end structure are renumbered to make the path shorter. This can be done in several ways and our choice is arbitrary, made by inspection (the choice should not be important as the result should only depend on the end points). The calculations were performed in VASP using the HSE06 functional, PAW pseudopotentials and a 500

eV cutoff energy. Due to computational limitations we only use $2\times2\times2$ k-points for these calculations, however from comparison with Γ-point calculations the effect of k-points on the calculated polarization is found to be minimal (see Figure 14). We do however find that some of the intermediate structures close to λ=0.5 become metallic when more than one k-point is used, and the polarisation can thus not be calculated for these structures. Instead we perform the calculations for all structures along the path using the Γ-point only and use the results to construct the path connecting the non-metallic points calculated with $2\times2\times2$ k-points. The spontaneous polarisation is found to be 67.8 and 68.3 μ C cm^{-2} for the $2\times2\times2$ and $1\times1\times1$ k-point meshes respectively for enargite.

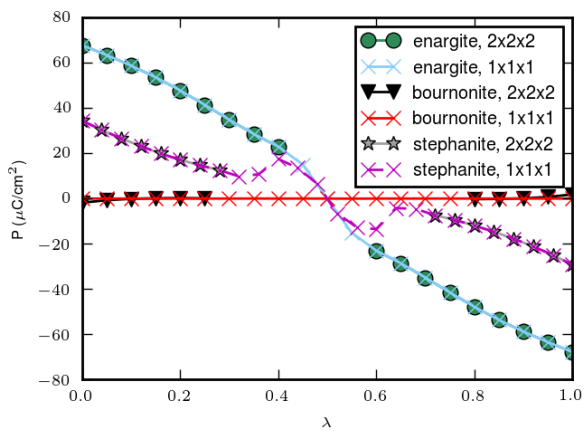

Figure 14: Calculated spontaneous polarisations of enargite (Cu_3AsS_4), stephanite (Ag_5SbS_4) and bournonite ($CuPbSbS_3$) using $1\times1\times1$ and $2\times2\times2$ k-points.

9 Energy barriers to switch direction of lattice polarisations

Figure 15 shows that the energy change along the paths used to calculate the spontaneous lattice polarisation. These provide an upper bound for the energy barrier for polarisation switching, however we note that since the path is not optimised (e.g. as in a nudged elastic band calculation) the real barrier is expected to be significantly lower.

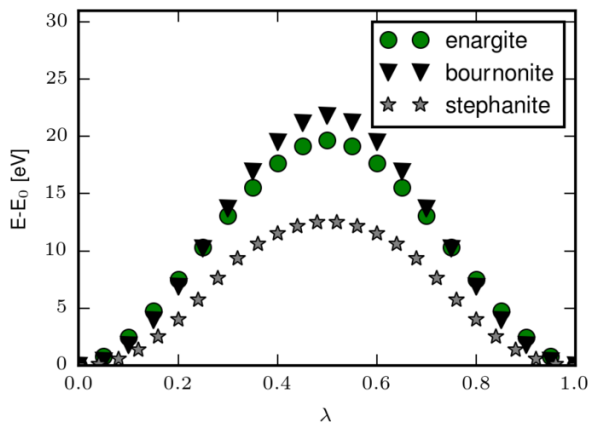

Figure 15: Energy barrier to switch the direction of lattice polarisation in enargite (Cu_3AsS_4), stephanite (Ag_5SbS_4) and bournonite ($CuPbSbS_3$).